Astronomy
&
Astrophysics

Chemical composition and evolutionary status of nine UV-bright stars in five globular clusters from VLT/UVES spectra[*,**,***]

G. Jasniewicz[1], P. de Laverny[2], M. Parthasarathy[3], A. Lèbre[1], and F. Thévenin[2]

[1] UMR 5024 CNRS/UMII, Université Montpellier II, CC 72, 34095 Montpellier Cedex 5, France
   e-mail: Gerard.Jasniewicz@graal.univ-montp2.fr
[2] Dpt. Cassiopée, UMR 6202, Observatoire de la Côte d'Azur, BP 4229, 06304 Nice Cedex 4, France
[3] Indian Institute of Astrophysics, Koramangala, Bangalore 560034, India

Abstract. We have derived the chemical composition of nine UV-bright stars belonging to five Galactic globular clusters of various metallicities ([Fe/H] from -1.0 to -2.4 dex). The analyses are based on high resolution spectra obtained with the UV-Visual Echelle Spectrograph (UVES) at VLT-UT2. The evolutionary status of the stars is assessed from the chemical analysis and location in the H-R diagram.
The star ID7 in NGC 5986 is confirmed as a bona fide post-asymptotic giant branch star (post-AGB) whereas the high-luminosity star ID6 has probably left the AGB before the third dredge-up. ZNG 1 in NGC 6712 shows an overabundance of sodium, oxygen, and silicon similar to overabundances we find in the UV-bright star ID6 in NGC 5986; both stars could be in a post-early-AGB (PEAGB) phase of evolution. The UV-bright star ZNG 7 in NGC 6218 seems to be an AGB star. The stars V-4 and ZNG 5 in NGC 6656 are in a post-horizontal-branch phase of evolution, with V-4 being significantly overabundant in heavy elements. The origin of these overabundances is discussed in the context of the evolutionary versus primordial scenario. The three UV-bright stars K 260, K 996 and K 1082 observed in the very metal-deficient globular cluster NGC 7078 are post-horizontal-branch stars, one of them being slightly enriched in s-elements but with a luminosity too low for third dredge-up to have occured. The abundance patterns of K 1082 in NGC 7078 seem to indicate the presence of mild diffusion and a radiative levitation process, already reported in the blue HB stars of M 13 (Behr et al. 1999, ApJ, 517, L135) and NGC 6752 (Moehler et al. 1999, A&A, 339, 537).

Key words. stars: abundances – stars : AGB and post-AGB – Galaxy: globular clusters : general

1. Introduction

UV-bright stars are found in several Milky Way globular clusters, but there are at most a few per cluster. The first survey was done by Zinn et al. (1972, ZNG) who introduced the term "UV-bright stars" for those lying above the horizontal branch (HB) and bluer than red giants. A first compilation of these stars was done by Harris et al. (1983). The contribution of UV-bright stars to globular cluster luminosities has been tackled by de Boer (1985, 1987).

In addition, observers distinguish among UV-bright stars those that are the supra-horizontal-branch stars (supra-HB) that are about one magnitude above the HB, and high-luminosity stars lying several magnitudes above the HB (see Sweigart et al.

1974). The presence/absence of supra-HB stars in globulars is strongly correlated with the presence/absence of hot HB stars (Zinn 1974; Moehler 2001).

The main question we address in this paper is: what is the evolutionary status of the UV-bright stars?

From a theoretical point of view, Dorman et al. (1993) show that there is a critical envelope mass ~ 0.05 $M_\odot$ for HB stars, above which the fuel supply is adequate to enable the evolution to reach the later stages of AGB evolution. The normal AGB sequence evolves through a thermal pulsing stage to a high post-AGB luminosity $\log L/L_\odot \gtrsim 3.5$.

Stars on this post-AGB branch are bona fide post-AGB stars (see Fig. 1 in Dorman et al. 1993). Dorman et al. (1993) use the appelation "extreme horizontal branch" (EHB) to refer to HB sequences of constant mass that do not reach the thermally pulsing stage on the AGB. These models evolve after core helium exhaustion into post-early AGB (PEAGB) stars, which leave the AGB before thermal pulsing, and AGB-manqué stars, which never reach the AGB. EHB stars have envelope masses that are too small to reach the end stages of normal AGB evolution. AGB-manqué stars are the fate of HB stars

with the less massive envelopes (<0.02 $M_\odot$ and $\log T_{\rm eff} > 4.3$) that do not support hydrogen shell burning.

Globular clusters with populous EHBs are expected to be deficient in post-AGB stars; however, they are expected to show a substantial population of less luminous ($1.8 < \log L/L_\odot < 3$) UV-bright stars, which can be either post-EHB stars or PEAGB stars. The population of post-EHB stars is expected to be about 15−20 percent of the population of EHB stars (Dorman et al. 1993).

We can suggest some answers to the question raised just above. The most luminous UV-bright stars can be PAGB stars; less luminous ones can be PEAGB or AGB manqué stars evolving from hot-HB stars, or evolved blue stragglers; mergers of stars; first ascent giants that have lost their outer envelopes, etc. Thus the location of UV-bright stars in the HR diagram is not sufficient at all for discriminating their origin, and high resolution spectroscopy is necessary for useful constraints (for example signatures of the third dredge-up, spectral binarity, etc.).

Only five UV-bright stars have detailed chemical composition determinations based on high resolution spectra: Barnard 29 in M 13 (Conlon et al. 1994; Moehler et al. 1998), ZNG 4 in M 13 (Ambika et al. 2004), ROA 24 in ω Cen (Gonzalez & Wallerstein 1994), ROA 5701 in ω Cen (Moehler et al. 1998), and ZNG 1 in M 10 (Mooney et al. 2001). To this list we can add the young planetary nebula K 648 in M 15 (Bianchi et al. 2001). These studies indicate that some UV-bright stars show evidence for third dredge-up and overabundance of carbon and s-process elements (for example ROA 24 in ω Cen and K 648 in M 15), while others show severe carbon deficiency, indicating that they left the AGB before the third dredge-up occured (for example ZNG 1 in M 10, ROA 5701 in ω Cen, Barnard 29 in M 13).

The chemical analysis of UV-bright stars must be done while keeping in mind the general chemical peculiarities (initially devoted to stars from the main sequence to the red giant branch) of the host clusters in the framework of evolutionary and/or primordial scenarios (see the review by Kraft 1994; and Sneden 1999). These discussions have stimulated investigations toward two directions: on one hand, deep extra-mixing mechanisms in giants, and on the other hand yields from contamination by AGB stars (Ventura et al. 2002). Combined scenarios are currently developed in papers by Denissenkov and collaborators (see Denissenkov & Herwig 2003), while accretion scenarios in globulars are progressing (Thoul et al. 2002).

Self-enrichment processes among globular clusters should also affect the abundance patterns of their most evolved stars (the UV-bright stars among them). In order to further constrain the evolutionary status of UV-bright stars and their chemical composition, we have undertaken high resolution spectroscopic observations in five clusters. Here we report the chemical abundance analysis performed on spectra obtained with the UVES instrument at VLT Unit-2, ESO, Chile. In Sect. 2 we list the selected targets and in Sect. 3 we describe the reduction of the high-resolution UVES spectra. Analysis of the spectra and location of the stars in the HR diagram are given in Sect. 4. Chemical analysis is done in Sect. 5 with concluding remarks in Sect. 6.

2. Selection of globular clusters and stars

2.1. Selection of globular clusters

The clusters NGC 5986, NGC 6218 (M 12), NGC 6656 (M 22), NGC 6712, and NGC 7078 (M 15) contain UV-bright star candidates and could be observed during our scheduled telescope time. The cluster metallicities cover the range between roughly −2 and −1 dex (see Table 1). Hereafter we list some published results on the HB morphology of the selected clusters and provide some discussion of the chemical abundance patterns of their stars in the framework of evolutionary or primordial scenarios.

– NGC 5986: the horizontal branch here is predominantly blue (Alves et al. 2001). According to Kravtsov et al. (1997) the luminosity function of the horizontal branch shows systematic changes as one goes from the central regions of the cluster to its periphery;
– NGC 6218 (M 12): the color–magnitude diagram (CMD) is very similar to the one for M 10 (Von Braun et al. 2002), exhibiting an extremely blue horizontal branch (very high value of the morphology parameter in Table 1);
– NGC 6656 (M 22): this cluster shows the anomalous abundance patterns of ω Cen (Norris & Freeman 1983). Giants display variations in Ca, Na, and Fe abundance, and these variations correlate with variations in CH and CN band strength (Lehnert et al. 1991). Brown & Wallerstein (1990) discuss the possibility that winds from massive WR stars or, more likely, cool supergiants provided self-enrichment during the star-formation period in M 22;
– NGC 6712: this cluster is a small and sparse system of intermediate metallicity, but is suspected to have been much more massive and concentrated at some early epoch of its history (Paltrinieri et al. 2001). The extension of the blue HB tail is small. The bulk of the horizontal branch stars populate the red side of the instability strip (Paltrinieri et al. 2001);
– NGC 7078 (M 15): this cluster shows an extended blue tail and a gap in the distribution of stars along the HB. Stellar rotation rates and photospheric compositions of HB stars vary strongly as a function of effective temperature (Behr et al. 2000). According to Sneden et al. (2000b), the large star-to-star scatter in [Na/Ca] observed in giants confirms the existence of large proton-capture abundance variations down to stellar luminosities comparable to the HB. Aikawa et al. (2001) argue that a deep mixing mechanism is probably responsible for the observed abundance anomalies.

2.2. The selection of stars

Most of the program stars in Table 2 were selected from the Zinn et al. (1972) and Harris et al. (1983) lists of UV-bright stars. Their cluster membership was checked from published proper motions and/or radial velocities, when available.

– NGC 5986: the stars labelled ID 6 and ID 7 in Alves et al. (2001) are yellow post-AGB candidates according to these authors.

Table 1. Selected globular clusters. $E(B - V)$, distances D from the sun and radial velocities V_R are from Harris (1996); [Fe/H] based on FeII lines is from Kraft & Ivans (2003), but from Harris (1996) for NGC 6656; ages are from Salaris & Weiss (2002). The HB morphology parameter $B2/B + R + V$ (Buonanno et al. 1997) is an estimator of the extension of the blue HB tail. Uncertainties are typically 0.05 in $E(B - V)$, 1 kpc in distance, 0.1 dex in [Fe/H], 1 Gyr in age and 0.7 km s^{-1} in radial velocity.

Ident	$E(B - V)$	D (kpc)	[Fe/H]	Age (Gyr)	V_R(km s^{-1})	$B2/B + R + V$
NGC 5986	0.27	10.4	−1.61		+88.9	0.52
NGC 6218	0.19	4.9	−1.34	12.5	−42.1	0.80
NGC 6656	0.34	3.2	−1.64	12.3	−148.9	0.28
NGC 6712	0.46	6.9	−1.10	10.4	−107.7	0.02
NGC 7078	0.09	10.3	−2.45	11.7	−107.5	0.43

Table 2. Program stars. References for the names (Col. 2) are the following: 1 – Alves et al. (2001); 2 – Zinn et al. (1972); 3 – Alcaino & Liller (1983); 4 – Kustner (1921). Column 3 gives the number of OBs used for each spectrum. For each OB the exposure time (in seconds) and S/N for each arm of the spectrograph (blue and red) are given in Cols. 4−6.

Ident.	Ref.	OBs	Expos.	S/N	S/N
		n	s	Blue	Red
NGC 5986 ID 6	1	1	1500	100	120
NGC 5986 ID 7	1	1	1800	100	120
NGC 6218 ZNG 7	2	1	2700	50	65
NGC 6656 V-4	3	1	1500	70	130
NGC 6656 ZNG 5	2	1	1500	110	120
NGC 6712 ZNG 1	2	1	3000	120	140
NGC 6712 ZNG 2	2	2	3000	60	80
NGC 6712 ZNG 4	2	2	3000	40	70
NGC 7078 K260	4	3	3000	70	95
NGC 7078 K996	4	2	3000	60	70
NGC 7078 K1082	4	5	3000	55	60

- NGC 6218 (M 12): ZNG 7 and ZNG 8 are UV-bright stars from (Zinn et al. 1972). Both are members of the cluster on the basis of radial velocities (Harris et al. 1983) proper motion measurements (Geffert et al. 1991). We excluded from our program the star ZNG 8 which has been recently observed by Klochkova & Samus (2001) with the 6-meter telescope at the Special Astrophysical Observatory (Caucasus).
- NGC 6656 (M 22): ZNG 5 and V-4 are members of the cluster on the basis of their proper motions according to Peterson & Cudworth (1994). Radial velocity measurements of V-4 (Côté et al. 1996) are in agreement with the systemic velocity of the cluster. Both stars belong to the list of Harris et al. (1983).
- NGC 6712: the stars ZNG 1, ZNG 2 and ZNG 4 were selected from Zinn et al. (1972). ZNG 1 and ZNG 4 are cluster members according to their proper motions (Cudworth 1988). The radial velocity of ZNG 1 (Webbink 1981) is in agreement with the velocity of the cluster.

- NGC 7078 (M 15): the stars K 260, K 996 and K 1082 are members on the basis of their radial velocities (Soderberg et al. 1999; Hesser & Nemec 1979) and proper motion measurements (Cudworth 1976). The star K 996 is a UV-bright star in the Zinn et al. (1972) list; all three stars are also in Harris et al. (1983).

3. The observations and the cluster membership of the program stars

3.1. UVES data reduction

The spectra were obtained with the UVES spectrograph (Dekker et al. 2000) attached to the second VLT unit (Kueyen telescope), from April to September 2002 (program ID 69.D-0081) (see Table 2 for details of the program). A total of 20 Observing Blocks (OBs) were obtained, corresponding to about 20 h of observation including overhead. The slit width used was 1″ corresponding to a spectral resolution of ≈40 000. The mean seeing during the observations was ∼1″. Two wavelength regions (4143−5213 Å and 5216−6213 Å) were observed simultaneously using the blue and red UVES arms. In order to estimate the S/N ratio of our data, we partitioned the blue and red wavelength region into bins of 1000 pixels, each pixel corresponding respectively to 13 Å and 16 Å. Within each bin i we calculated the average F_i of the relative flux, the standard deviation σ_i, and the ratio F_i/σ_i. The S/N ratio, which is a function of λ, was estimated from the *continuum* of the curve F_i/σ_i versus i. Among our program stars the S/N ratio of a single OB varies from 40 to 120 in the blue region, and 60 to 140 in the red.

The UVES Data Reduction Standard Pipeline (Ballester et al. 2000) was used for the reduction of the spectra. A detailed data treatment was then performed using MIDAS facilities. For each star and given spectral range, the images were first averaged and the resulting spectrum was binned by three pixels as well as corrected to the local standard of rest. At this step, each pixel corresponds to 0.0393 Å in the blue and 0.0478 Å in the red. Finally, each spectrum was normalized with respect to the stellar continuum of energy.

Table 3. General data for the program stars. References for the photometry are the same that in Table 1; following references are: (5) Harris et al. (1983); (6) Cote et al. (1996); (7) Peterson & Cudworth (1994); (8) Cudworth (1988); (9) Sandage & Smith (1966); (10) Cudworth (1976); (11) Buonanno et al. (1983); (12) Battistini et al. (1985). We estimate the probable error on radial velocities to be ± 0.7 km s^{-1}.

Ident.	V	$(B-V)$	Ref.	V_R (km s^{-1})
				This work
NGC 5986 ID 6	12.652	0.303	1	+100.8
NGC 5986 ID 7	12.755	0.553	1	+92.5
NGC 6218 ZNG 7	13.11	0.78	5	−41.1
NGC 6656 V-4	12.4	0.95	6	−147.7
NGC 6656 ZNG 5	12.57	0.48	7	−139.0
NGC 6712 ZNG 1	13.33	0.33	8	−116.4
NGC 6712 ZNG 2	13.92	0.63	9	−25.5
NGC 6712 ZNG 4	14.06	0.53	8	+20.1
NGC 7078 K260	13.90	0.73	10	−96.4
NGC 7078 K996	14.31	0.09	11	−105.5
NGC 7078 K1082	15.02	0.25	12	−111.3

3.2. Cluster membership check of the program stars

Radial velocities were derived by cross-correlation of observed spectra (obtained in the blue arm) with synthetic spectra (see Table 3). The stars ZNG 2 and ZNG 4 in NGC 6712 are clearly not members of the cluster on the basis of their radial velocity measurements. Hence, these two stars have been removed from our sample. The memberships of the nine remaining program stars are confirmed.

4. Stellar parameters and HR diagram

4.1. Stellar parameters

For the sample, we estimated the effective temperatures T_{eff} from available photometric colours and used them as starting values for the spectroscopic study. Temperatures were computed from $(B-V)_0$ colors, using the calibration by Houdashelt et al. (2000) for the cooler stars $T_{\text{eff}} \leq 6500$ K and by Flower (1996) for the hotter ones. Bolometric corrections were also calculated for each star from these papers.

Derived temperatures have an accuracy controlled by forcing the abundances deduced from the line equivalent widths to be independent of the excitation potential of the lines used. The convergence of the procedure depends strongly on the adopted surface gravity g. Consequently, the abundance analyses were iterated by deriving the T_{eff} and g until the element abundances were independent of the line excitation potential and neutral and ionized lines gave the same abundance. The final values of T_{eff} and $\log g$ are given in Table 4. The spectroscopic T_{eff} are generally different from the photometric ones except for the coolest stars. The spectroscopic surface gravities have been checked with the evolved surface gravities when adopting a

mean mass of 0.6 $M_{\odot}$ for the observed post-AGB candidate stars, and no important difference has been found. We estimate that the accuracy of our derived T_{eff}, [Fe/H] and $\log g$ are respectively 500 K, 0.2 dex and 0.5 dex for the hottest stars and 250 K, 0.2 dex and 0.3 dex for the coolest ones.

The microturbulence ζ_{turb} was obtained by fitting the plateau of the curve of growth of chemical elements. The estimate of this parameter is very important because for the program stars it has been very difficult to measure equivalent width of very weak lines which do not depend on it. The microturbulence velocity was assumed to be depth-independent with an uncertainty of about 0.3 km s^{-1}.

For all program stars, it was necessary to add a macroturbulence velocity parameter to the broadening function in order to improve the fit to the observed lines. The uncertainty on this macroturbulence velocity is around 1 km s^{-1}. No rotational broadening is seen for any of the program stars except one, and we assume a low value of the rotational velocity for the rest (1 km s^{-1}). However, for NGC 6656 ZNG5 a rotational velocity of 15 km s^{-1} (± 1 km s^{-1}) was adopted to fit the observed profile.

4.2. The HR diagram

Luminosities of the stars have been calculated by means of published photometry (Table 3), cluster distance (Table 1), and bolometric corrections from Houdashelt et al. (2000) and Flower (1996). Using the effective temperatures and luminosities deduced in this work, we have compared the location in the HR diagram of the observed stars with evolutionary tracks computed by Dorman et al. (1993). In Fig. 1, the Zero Age Horizontal Branch (ZAHB) marks the position where the HB stars have settled down and started to quietly burn helium in their cores. As in Fig. 2 of Moehler (2001) we have also plotted the Terminal-Age Horizontal Branch (TAHB) where helium is exhausted in the core of an HB star (central helium fraction <0.0001). The ZAHB, TAHB, and other main loci are placed in Fig. 1 for [Fe/H] = −1.48, helium composition of 0.247 and a core mass of 0.485 $M_{\odot}$ (see Dorman et al. 1993). We have checked that these loci are not modified a lot when using Dorman's models with [Fe/H] = −2.26.

Except for NGC 7078 K1082, lying very close to the HB (label 9 in Fig. 1), all the program stars appear to be supra-HB stars and/or high luminosity stars. The evolutionary stage of each star is discussed in the next section.

5. Chemical analysis of the program stars

5.1. The chemical abundances

The wavelength range covered by our spectra is 4143−5213 Å and 5216−6213 Å. Unfortunately our spectra do not extend up to 7500 Å in order to provide carbon abundance from the multiplet CI near 7115 Å and nitrogen abundance from the triplet at 7450 Å.

The chemical abundances were derived by fitting synthetic spectra to the observed profiles with the set of stellar parameters given in Table 4. Synthetic spectra were computed with
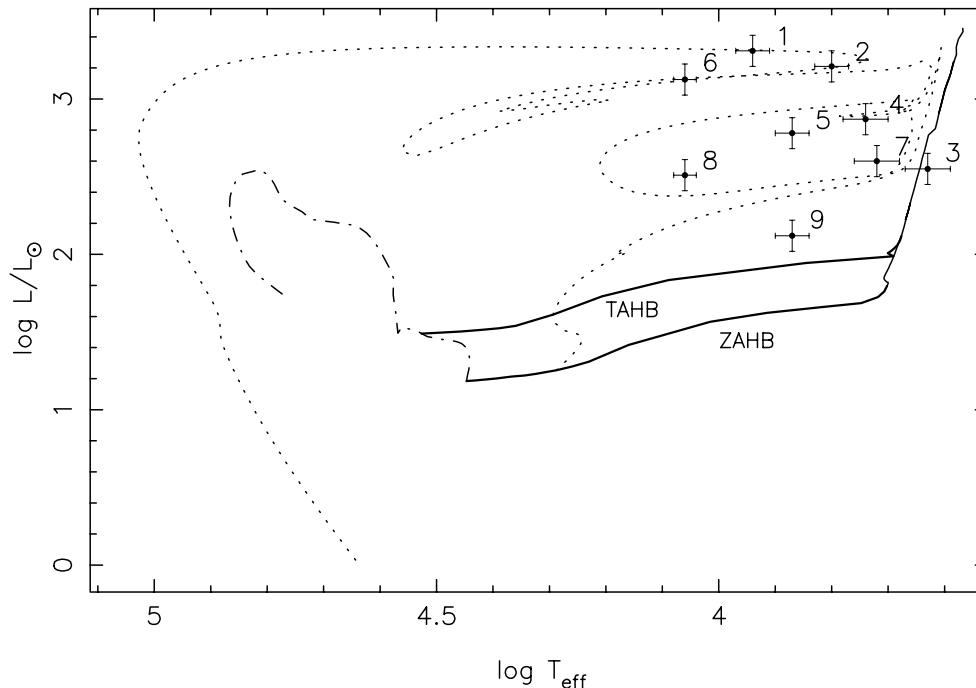
Fig. 1. The HR diagram with the program stars. All theoretical evolutionary sequences are from Dorman et al. (1993) and drawn for [Fe/H] = −1.48, a core mass of 0.485 $M_\odot$ and a helium composition of 0.247. Solid thick lines: Zero Age HB (ZAHB) and Terminal Age HB (TAHB) sequences. The three post-HB evolutionary sequences correspond to three total masses (i.e. core + envelope) at the ZAHB: 0.488 $M_\odot$ (dotted-dashed: AGB-manqué sequence), 0.520 $M_\odot$ (dotted line: post-early AGB sequence), 0.900 $M_\odot$ (solid thin line: AGB sequence). The program stars are labelled according to Col. 2 from Table 4.

the assumption of LTE using a new version of the code MOOG written by C. Sneden (1973)[1]. Model atmospheres were interpolated in a grid of Kurucz (1993) ATLAS9. Atomic lines used for the abundance determination have log gf from VALD2 (Kupka et al. 1999). Most metallic lines are from Thévenin (1989, 1990). We used the work of Lambert et al. (1996) for iron line selection. For the coolest stars where molecules can exist, we have not detected CN and CH molecular lines at 4216 and 4300 Å. Thus we have not estimated C and N abundances. Finally, the resulting mean abundances are given in Table 5 with respect to the solar value (Anders & Grevesse 1989), except for iron, where we have adopted 7.46 (Holweger 1979). The mean abundances are also plotted in Fig. 2. For hot stars (typically $T_{\rm eff} \sim 10\,000$ K, log g = 2.5, $\zeta_{\rm turb}$ = 2.5 km s^{-1}) the quadratic errors take into account the probable errors (see Sect. 4.1) on $T_{\rm eff}$, log g, $\zeta_{\rm turb}$, [Fe/H] and $V_{\rm macro}$ and they are respectively 0.28 dex, 0.37 dex and 0.49 dex for [O/Fe], [α elements/Fe] and [s elements/Fe]. For cool stars (typically $T_{\rm eff} \sim$ 6500 K, log g = 1.0, $\zeta_{\rm turb}$ = 2.5 km s^{-1}) these quadratic errors are 0.28 dex, 0.25 dex and 0.28 dex. Details of abundances line by line are arranged in an electronic table (Table 6) available at the CDS. Notes on individual objects are given in the Appendix. Heavy elements are discussed globally in Sect. 5.2.

5.2. Barium, europium, and other heavy elements

Reyniers & van Winckel (2003) have detected elements beyond the Ba-peak in VLT+UVES spectra of field post-AGB stars.

We have searched in vain for WII, YbII, and GdII lines in our spectra, and thus concentrated our effort to less heavy elements. In their search for evidence for primordial abundance variations in globulars, Sneden et al. (1997a) emphasize that the ratio Ba/Eu is a sensitive test of the relative importance of the s- or r-process origin of these elements. Thus this ratio is often taken as a measure of the relative contributions in the primordial material of evolved low-to-intermediate mass stars and of the supernovae. We have plotted data for all the program stars from Table 7 in Fig. 3 in the plane [Ba/Eu] versus [Ca/H] in the manner of Fig. 7 from Sneden et al. (1997a). We have marked in Fig. 3 the total solar abundance ratio ([Ba/Eu] ≡ 0), the solar system r-process value of −0.69 dex (Käppeler et al. 1989), and the predicted value for a pure s-process (Malaney 1987b). From Fig. 3 we can deduce some interesting results:

– The s-process elements enhancement in spectra of ID 7 in NGC 5986 is slightly lower than that of the post-AGB star ROA 24 in ω Centauri, which also shows overabundance of carbon (Gonzalez & Wallerstein 1992). The luminosity of ROA 24 is 1800 $L_\odot$, similar to ID 7. The Ba and La abundances of ID 7 in NGC 5986 show slight overabundances. The [La/Fe] abundance in this star is similar to that found in the giant stars of M 4 (Ivans et al. 1999). However the [Ba/Eu] ratio is −0.49 dex, similar to that found in metal-poor halo giants indicating r-process origin of heavy elements. Unfortunately, there is no chemical composition study of giants in NGC 5986 to compare with the heavy element abundances of ID 7 in NGC 5986. In order to further understand the heavy element abundance pattern of ID 7 in NGC 5986 (evolutionary or primordial) we need

---

[1] http://verdi.as.utexas.edu/moog.html
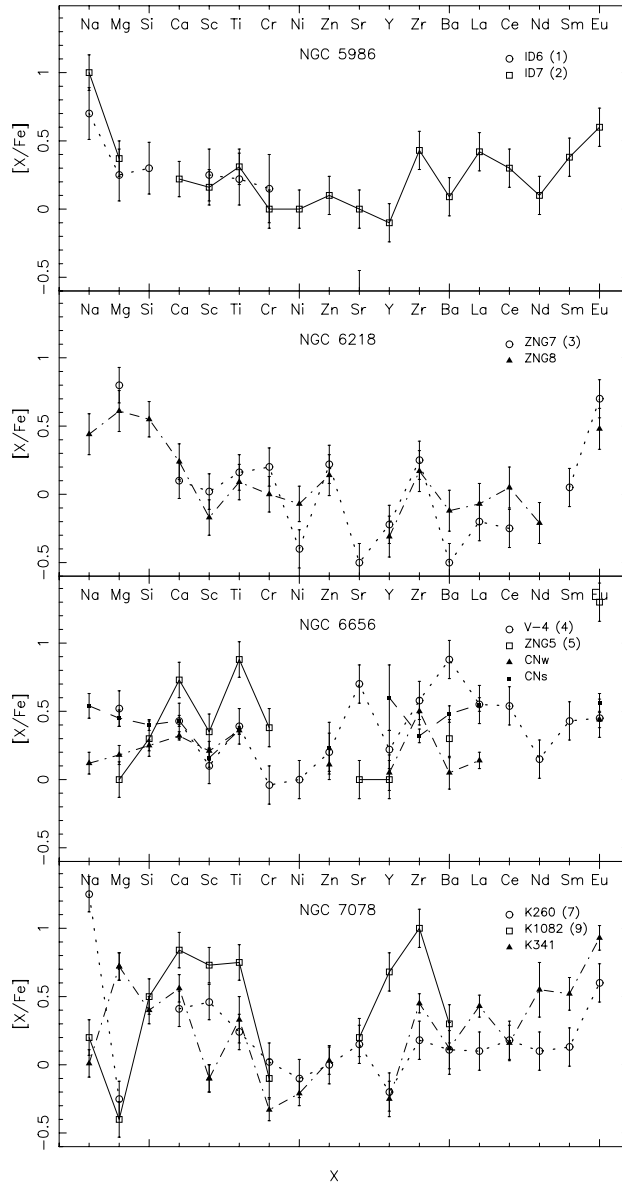
Fig. 2. Mean abundances [X/Fe] and error bars of some UV-bright stars observed in this work (see Table 5). The number in parentheses is the serial number defined in Col. 2 from Table 4. NGC 6218: abundances for ZNG 8 are from Klochkova & Samus (2001). NGC 6656: CNw and CNs are the mean abundances from Brown & Wallerstein (1992) respectively for the CN-weak and CN-strong giants. NGC 7078: abundances for K 341 are from Sneden et al. (1997a, 2000a,b).

to determine the heavy element abundances in red giant branch and AGB stars of NGC 5986.

– The heavy element abundances and [Ba/Eu] values of ZNG 7 (−1.20, this work) and of ZNG 8 (−0.60, Klochkova & Samus 2001) in NGC 6218 play in favour of a pure r-process origin in the early chemical history of the globular cluster NGC 6218. But this result has to be confirmed by chemical analyses of other giant stars in this cluster.

– From the analysis of spectra of three giants in NGC 7078 Sneden et al. (2002b) find [Ba/Eu] = −0.87, which is substantially below the total solar ratio, indicating that the heavy

elements in this cluster are of r-process origin. The heavy element abundances of K 260 in NGC 7078 are in agreement with the ones found in NGC 7078 giants (Sneden et al. 1997a). The neutron-capture elements in NGC 7078 giants and in K 260 (see Fig. 3) reflect a nucleosynthesis history much more dominated by the r-process than is material in the solar system.

– Brown & Wallerstein (1992) derived Ba, La, and Eu abundances in several CN-weak and CN-strong giants in NGC 6656 (see Table 7). The CN-strong giants seem to show overabundance of heavy elements. The [Ba/Eu] ratio in CN-strong giants is −0.08 dex whereas in CN-weak giants it is −0.39 dex. In the star V-4 in NGC 6656 we find significant overabundance of heavy elements (Table 7). The [Ba/Eu] = +0.43 is significantly higher than the solar value. The heavy element abundance pattern of V-4 in NGC 6656 is similar to that in NGC 6121 giants for which [Ba/Eu] = +0.25 (see Table 7). One possibility is that V-4 has gone through third dredge-up. Subsequent mixing would have enhanced s-process products at the surface as for the UV-bright stars V1 and ROA24 of ω Cen (Gonzalez & Wallerstein 1994). The heavy element abundance pattern of V-4 in NGC 6656 (Fig. 4) indicates a neutron flux $\tau_0 \sim 0.6$ (see Malaney 1987; Gonzalez & Wallerstein 1994).

Another possibility is that the overabundance of V-4 in NGC 6656 is not due to third dredge-up. The Ba and La enhancements in this star and M 4 (Ivans et al 1999) are not the result of a slow neutron-capture synthesis occuring in the stars themselves, but could be signatures of primordial enrichments of the material from which V-4 and M 4 giants are formed. The giants in the clusters NGC 6287, NGC 6293, and NGC 6541 also show the s-process elements Ba and La slightly enhanced compared to the field metal-poor stars (Lee & Carney 2002).

Among halo field giants and giants in globulars the [Eu/Fe] ranges from +0.3 to +0.5, which is in agreement with our finding for V-4 in NGC 6656. The study of heavy elements in globulars by Brown & Wallerstein (1992) is limited to seven giants in NGC 6656 for which the abundances are not well determined according to the authors. However if we trust their abundance patterns, we can hypothesize the following scenario: for their CN-weak giants, [Ba/Eu] = −0.39 is close to the solar-system r-process value. But the ratio [Ba/Eu] = −0.08 for their CN-strong stars is nearly the total solar-system $r + s$ value (=0.0). Thus the CN-strong stars could be enhanced by s-elements from primordial matter, but not the CN-weak stars, because the protocluster gas cloud was not homogeneous during the epoch of low-mass star formation. Consequently V-4 in NGC 6656 could be enhanced in s-elements with regard to the CN-strong stars due to dredge-up s-processing. Moreover, ten red giant stars of NGC 6656 observed by Lehnert et al. (1991) display variations in Ca, Na, and Fe and show a calcium enhancement that is accompanied by enhancements of C and possibly N. Since Ca is not thought to be produced in the interiors of low-mass red giants, Lehnert et al. (1991) also argue that the cause of these variations may be primordial. Our results concerning ZNG 5 (Sect. 5.4.2) support this hypothesis.

Further study of RGB and AGB stars of NGC 6656 with multi-fiber spectrographs such as GIRAFFE installed at the ESO-VLT will probably help elucidate the evolutionary and

Table 4. Atmospheric parameters and luminosities of the program stars as derived in this work. A serial number valid for the remainder of the paper is attributed to each star. We adopt $\log \epsilon = 7.46$ for the solar iron abundance (Holweger 1979).

Identifier	Label	$L/L_\odot$	$T_{\rm eff}$ (K)	$\log g$	$\zeta_{\rm turb}$ (km s^{-1})	[Fe/H]	$V_{\rm macro}$ (km s^{-1})	$V_{\rm rot}$ (km s^{-1})
NGC 5986 ID 6	1	2000	8750	2.0	2.5	−1.70	4.0	1.0
NGC 5986 ID 7	2	1600	6300	1.0	2.5	−1.80	8.0	1.0
NGC 6218 ZNG 7	3	350	4240	0.6	2.6	−1.80	4.0	1.0
NGC 6656 V-4	4	740	5500	1.4	4.7	−1.80	14.0	1.0
NGC 6656 ZNG 5	5	600	7450	1.4	2.6	−1.60	15.0	15.0
NGC 6712 ZNG 1	6	1300	11 500	2.5	2.5	−1.20	1.0	1.0
NGC 7078 K260	7	400	5250	1.0	4.2	−2.50	12.0	1.0
NGC 7078 K996	8	330	11 500	2.5	2.5	−2.10	2.0	1.0
NGC 7078 K1082	9	130	7500	2.4	2.5	−2.10	5.0	1.0

Table 5. Mean LTE abundances [X/Fe] with respect to the Sun for some elements. The label of the star is the same as in Table 4. Abundances are given line by line in Table 6. For the solar abundances we adopt Anders & Grevesse's values (1989) except for iron (see Sect. 5.1).

NGC	5986	5986	6218	6656	6656	6712	7078	7078	7078
Star	ID 6	ID 7	ZNG 7	V-4	ZNG 5	ZNG 1	K 260	K 996	K 1082
Label	1	2	3	4	5	6	7	8	9
[Fe/H]	−1.70	−1.80	−1.80	−1.80	−1.60	−1.20	−2.50	−2.10	−2.10
2 HeI	−0.40	−0.80	–	–	–	–	–	–	–
8 OI	+0.65	–	–	–	–	+0.40	–	–	–
11 Na	+0.70	>1.0	–	–	–	+0.65	+1.25	–	+0.20
12 MgII	+0.25	+0.37	+0.80	+0.52	+0.00	+0.00	−0.25	−0.70	−0.40
14 SiII	+0.30	–	–	–	+0.30	+0.60	–	−0.15	+0.50
20 CaI	–	+0.22	+0.10	+0.43	+0.73	–	+0.41	–	+0.84
21 ScII	+0.25	+0.16	+0.02	+0.10	+0.35	–	+0.46	–	+0.73
22 TiII	+0.22	+0.31	+0.16	+0.39	+0.88	−1.10	+0.24	–	+0.75
24 CrII	+0.15	+0.00	+0.20	−0.04	+0.38	−0.13	+0.02	–	−0.10
28 NiI	–	+0.00	−0.40	+0.00	–	–	−0.10	–	–
30 ZnI	–	+0.10	+0.22	+0.20	–	–	+0.00	–	–
38 SrII	−0.70	+0.00	−0.50	+0.70	+0.00	–	+0.15	–	+0.20
39 YII	–	−0.10	−0.22	+0.22	+0.00	–	−0.20	–	+0.68
40 ZrII	–	+0.43	+0.25	+0.58	–	–	+0.18	–	+1.00
56 BaII	–	+0.09	−0.50	+0.88	+0.30	–	+0.11	–	+0.30
57 LaII	–	+0.42	−0.20	+0.55	–	−0.10	+0.10	–	–
58 CeII	–	+0.30	−0.25	+0.54	–	–	+0.18	–	–
60 NdII	–	+0.10	–	+0.15	–	–	+0.10	–	–
62 SmII	–	+0.38	+0.05	+0.43	–	–	+0.13	–	–
63 EuII	–	+0.60	+0.70	+0.45	+1.30	–	+0.60	–	–

primordial scenarios in NGC 6656 and to compare this cluster with M 4.

6. Conclusions

By means of a detailed chemical analysis and study of their location in the HR diagram, the evolutionary status of nine UV-bright stars has been suggested (see also the notes on individual objects given in the electronic Appendix):

– ID7 in NGC 5986 could be a bona fide post-AGB star having probably experienced the third dredge-up.
– ZNG 7 in NGC 6218 seems to be an AGB star.

Table 6. LTE abundances [X/Fe] with respect to the sun for some elements. Values followed by *w* and *s* respectively are related to weak and saturated line. Some abundance determinations, marked COG, have been performed through a Curve of Growth technique. Only the first lines of the table are given hereafter. The full table is available in electronic form at the CDS.

	NGC:	5986	5986	6218	6656	6656	6712	7078	7078	7078
	Star:	ID 6	ID 7	ZNG 7	V-4	ZNG 5	ZNG 1	K 260	K 996	K 1082
Element	Line									
2 HeI	4471.5	−0.60	−0.70	–	–	–	–	–	–	–
	5875.6	−0.20	−0.90	–	–	–	–	–	–	–
8 OI	4368.24	+0.65	–	–	–	–	–	–	–	–
	6156.0	+0.65	–	–	–	–	+0.40	–	–	–
	6156.8	+0.65	–	–	–	–	+0.40	–	–	–
	6158.2	+0.65	–	–	–	–	+0.40	–	–	–

– NGC 6656 V-4, NGC 6656 ZNG 5, NGC 7078 K 260, NGC 7078 K 996, and NGC 7078 K 1082 are post-HB stars.
– NGC 5986 ID6 and NGC 6712 ZNG 1 are very luminous but are not overabundant in s-elements. These stars could be PEAGB stars (see Dorman et al. 1993) which leave the AGB before thermal pulsing.

The star NGC 7078 K 1082 shows possible signatures of diffusion and radiative levitation of elements in its spectra similar to those found in the post-HB star ZNG4 in M 13 (Ambika et al. 2004), and in the BHB stars in M 13 (Behr et al. 1999) and in NGC 6752 (Moehler et al. 1999).

The star NGC 6656 V-4 shows a significant overabundance of s-process elements but is not luminous enough to be in a post-AGB phase. This star could have suffered a third dredge-up episode, or has been enriched in somewhat way (binarity or primordial scenario). High-resolution spectra of red giant stars (both first-ascent giant branch and AGB) in NGC 6656 are needed.

The program stars ID6 and ID7 in NGC 5986, ZNG 1 in NGC 6712 and K 260 in NGC 7078 are overabundant in sodium. ID6 and K 260 differ by a factor of 5 in luminosity. Large variations and high sodium abundances have also been detected in red giants of NGC 2808 (Carretta et al. 2003) and turnoff stars in NGC 6397 (Thévenin et al. 2001). These variations are understood by these authors as being of primordial origin.

The overabundance of oxygen in NGC 6712 ZNG 1 and in NGC 7078 K 260 indicates that these two stars have not gone through a complete CNO cycle. They may have gone through the CN cycle but not through the ON cycle. They have left the AGB before the third dredge-up. It also indicates that the overabundance of Na in these two stars supports the idea that O-Na and Mg-Al correlations in the abundances of globular cluster stars is not due to deep mixing but to some external mechanism. The deep mixing scenario seems to be no longer valid on the basis of recent investigations among main sequence stars in globulars: there is a CN-CH anticorrelation in main sequence stars of 47 Tuc (Harbeck et al. 2003), abundance variations among light elements in stars near the main-sequence turnoff of M 5 (Ramirez & Cohen 2003), and an O-Na

Table 7. Heavy element abundances in six of the UV-bright stars observed in this work. The mean values for globular cluster giants are from: Brown & Wallerstein (1992) for NGC 6656 (CNs and CNw mean respectively CN-strong and CN-weak stars); Sneden et al. (1997a, 2000a,b), Armosky et al. (1994) for NGC 7078; Ivans et al. (1999) for NGC 6121 (M 4); Ivans et al. (2001), Armosky et al. (1994) for NGC 5904 (M 5); Lee & Carney (2002), for NGC 6287, NGC 6293 and NGC 6541. Probable errors for these data (~0.1 dex) are given in the quoted papers. The mean values for the field metal-poor stars concern eight stars with $-2 <$ [Fe/H] < -1 from the list of Gratton & Sneden (1991, 1994).

	[Ba/Fe]	[La/Fe]	[Eu/Fe]	[Ba/Eu]
UV-bright stars				
(this work)				
NGC 5986 ID7	+0.11	+0.42	+0.60	−0.49
NGC 6656 V-4	+0.88	+0.55	+0.45	+0.43
NGC 6656 ZNG5	+0.30	–	+1.30	−1.00
NGC 6218 ZNG7	−0.50	−0.20	+0.70	−1.20
NGC 7078 K260	+0.11	+0.10	+0.60	−0.49
NGC 7078 K1082	+0.30	–	–	–
Globular giants				
NGC 5904	+0.16	+0.02	+0.43	−0.27
NGC 6121	+0.60	+0.45	+0.35	+0.25
NGC 6287	+0.39	+0.28	+0.45	−0.06
NGC 6293	+0.00	+0.15	+0.42	−0.42
NGC 6541	+0.23	+0.13	+0.31	−0.08
NGC 6656 CNw	+0.05	+0.14	+0.44	−0.39
NGC 6656 CNs	+0.48	+0.55	+0.56	−0.08
NGC 7078	+0.00	+0.34	+0.89	−0.87
Field metal-				
poor stars	−0.08	−0.11	+0.29	−0.37

anticorrelation in unevolved stars in NGC 6752 (Gratton et al. 2001) and M 71 (Ramirez & Cohen 2002). A most likely origin
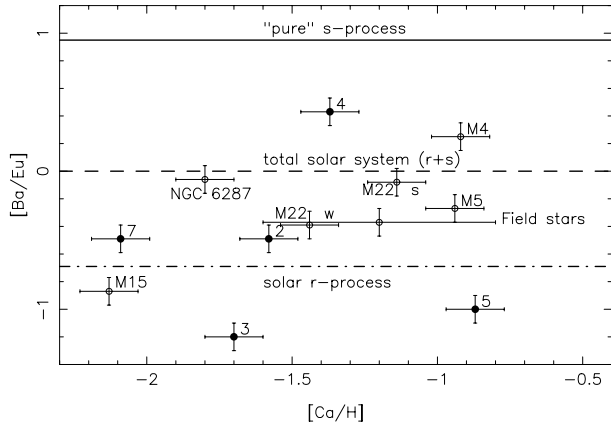
Fig. 3. This plot is adapted from Fig. 7 in Sneden et al. (1997a). The [Ba/Eu] values are taken from our Table 7. Solid line: pure s-process (see Malaney 1987b, $\tau_0 = 1.5$ mbarn^{-1} and neutron density of 10^8 cm^{-3}). Dashed line: total solar-system (r+s). Dotdashed line: solar r-process ([Ba/Eu] = -0.69, Käppeler et al. 1989). The program stars are plotted with a filled circle; the numbers of stars are the same as in Fig. 1. The mean values for giant stars in M 4 (NGC 6121), M 5 (NGC 5904), M 15 (NGC 7078) and M 22 (NGC 6656) are plotted with an open circle and error bars of 0.1 dex, and retrieved from the references given in Table 7 (s signifies the CN-strong and w the CN-weak stars). For the field metal-poor stars, the horizontal error bar reproduces the range $-1.6 <$ [Ca/H] < -0.8 corresponding to the eight stars with $-2.0 <$ [Fe/H] < -1.0 in the list of Gratton & Sneden (1991, 1994).
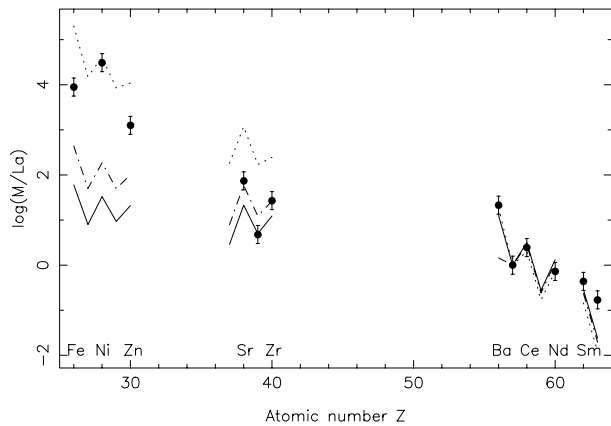
Fig. 4. The s-elements abundances (M/La) versus the atomic number Z for NGC 6656 V-4. The theoretical lines of s-process abundance patterns are taken from Malaney (1987a) for neutron density of 10^8 cm^{-3}: the dotted line, dotted-dashed line and full line corresponds respectively to a mean neutron exposure τ_0 equal to 0.1, 0.3 and 0.6 mbarn^{-1}. The theoretical lines and observations match precisely at $Z = 57$ by definition as in Fig. 14 in Gonzalez & Wallerstein (1994).

of these abundance anomalies and correlations among main sequence stars is pollution by material processed in earlier generation of AGB stars of intermediate mass (Ventura et al. 2002). However recent work on surface abundance evolution in extremely metal-poor intermediate-mass stars by Denissenkov & Herwig (2003) seems to raise some difficulty with the primordial scenario.

References

Aikawa, M., Fujimoto, M. Y., & Kato, K. 2001, ApJ, 560, 937
Alcaino, G., & Liller, W. 1983, AJ, 88, 1330
Alves, D. R., Bond, H. E., & Onken, C. 2001, AJ, 121, 318
Ambika, S., Parthasarathy, M., Aoki, W., et al. 2004, A&A, 417, 293
Anders, N., & Grevesse, E. 1989, Geochim. Cosmochim. Acta, 53, 197
Armosky, B. J., Sneden, C., Langer, G. E., & Kraft, R. P. 1994, AJ, 108, 1364
Battistini, P., Bregoli, G., Fusi Pecci, F., Lolli, M., & Epps Bingham, E. A. 1985, A&AS, 61, 487
Behr, B. B., Cohen, J. G., McCarthy, J. K., & Djorgovski, S. G. 1999, ApJ, 517, L135
Behr, B. B., Cohen, J. G., & McCarthy, J. K. 2000, ApJ, 531, L37
Bianchi, L., Bohlin, R., Catanzaro, G., Ford, H., & Manchado, A. 2001, AJ, 122, 1538
Brown, J. A., & Wallerstein, G. 1992, AJ, 104, 1818
Brown, J. A., Wallerstein, G., & Oke, J. B. 1990, AJ, 100, 1561
Buonanno, R., Buscema, G., Corsi, C. E., Iannicola, G., & Fusi Pecci, F. 1983, A&AS, 51, 83
Buonanno, R., Corsi, C. E., Bellazzini, M., Ferraro, F. R., & Fusi Pecci, F. 1997, AJ, 113, 706
Cacciari, C., Caloi, V., Castellani, V., & Fusi Pecci, F. 1984, A&A, 139, 285
Carretta, E., & Gratton, R. G. 1997, A&AS, 121, 95
Carretta, E., Bragaglia, A., Cacciari, C., & Rossetti, E. 2003, A&A, 410, 143
Conlon, E. S., Dufton, P. L., & Keenan, F. P. 1994, A&A, 290, 897
Coté, P., Pryor, C., McClure, R. D., Fletcher, J. M., & Hesser, J. E. 1996, AJ, 112, 574
Cudworth, K. M. 1976, AJ, 81, 519
Cudworth, K. M. 1988, AJ, 96, 105
D'Antona, F., Caloi, V., Montalbán, J., et al. 2002, A&A, 395, 69
de Boer, K. S. 1985, A&A, 142, 321
de Boer, K. S. 1987, in Conference on faint blue stars, 2nd, ed. A. G. D. Philip, D. S. Hayes, & J. W. Liebert, IAU Coll., 95
Dekker, H., D'Odorico, S., Kaufer, A., Delabre, B., & Kotzlowski, H. 2000, Proc. Conf. SPIE 4008-61
Denissenkov, P. A., & Herwig, F. 2003, ApJ, 590, L99
Dorman, B., Rood, R. T., & O'Connell, R. W. 1993, ApJ, 419, 596
Flower, P. J. 1996, ApJ, 469, 355
Geffert, M., Tucholke, H.-J., Georgiev, T. B., & LeCampion, J.-F. 1991, A&AS, 91, 487
Gonzalez, G., & Wallerstein, G. 1992, MNRAS, 254, 343
Gonzalez, G., & Wallerstein, G. 1994, AJ, 108, 1325
Gratton, R. G., & Sneden, C. 1991, A&A, 241, 501
Gratton, R. G., & Sneden, C. 1994, A&A, 287, 927
Gratton, R. G., Bonifacio, P., Bragaglia, A., et al. 2001, A&A, 369, 87
Harbeck, D. S., Graeme, H., & Grebel, E. K. 2003, AJ, 125, 197
Harris, H. C., Nemec, J. M., & Hesser, J. E. 1983, PASP, 95, 256
Harris, W. E. 1996, AJ, 112, 1487
Harris, W. E., Racine, R., & de Roux, J. 1976, APJS, 31, 13
Hesser, J. E., & Nemec, J. M. 1979, PASP, 91, 358

Holweger, H. 1979, Les éléments dans l'Univers, Proc. 22nd Liège Intern. Astrophys. Colloq., Université de Liège, 11

Houdashelt, M. L., Bell, R. A., & Sweigart, A. V. 2000, AJ, 119, 1448

Ivans, I. I., Sneden, C., Kraft, R. P., et al. 1999, AJ, 118, 1273

Ivans, I. I., Kraft, R. P., Sneden, C., et al. 2001, AJ, 122, 1438

Käppeler, F., Beer, H., & Wisshak, K. 1989, Rep. Prog. Phys., 52, 945

Klochkova, V. G., & Samus, N. N. 2001, A&A, 378, 455

Kraft, R. P. 1994, PASP, 106, 553

Kraft, R. P., & Ivans, I. I. 2003, PASP, 115, 143

Kraft, R. P., Sneden, C., Smith, G. H., et al. 1997, AJ, 113, 279

Kravtsov, V. V., Pavlov, M. V., Samus, N. N., et al. 1997, AZh, 23, 5

Kupka, F., Piskunov, N., Ryabchikova, T. A., Stempels, H. C., & Weiss, W. W. 1999, A&AS, 138, 119

Kurucz, R. L. 1993, CD-ROMs, ATLAS9 Stellar Atmospheres Programs (Cambridge: Smithsonian Astrophys. Obs.)

Kustner, F. 1921, VeBon, 15, 1

Lambert, D., Heath, J. A., Lemke, M., & Drake, J. 1996, ApJS, 103, 183

Langer, G. E., & Hoffman, R. D. 1995, PASP, 107, 1177

Langer, G. E., Hoffman, R. E., & Zaidins, C. S. 1997, PASP, 109, 244

Lee, J. W., & Carney, B. W. 2002, AJ, 124, 1511

Lehnert, M. D., Bell, R. A., & Cohen, J. G. 1991, ApJ, 367, 514

Malaney, R. A. 1987a, Ap&SS, 137, 251

Malaney, R. A. 1987b, ApJ, 321, 832

Mathis, J. S., & Lamers, H. J. G. L. M. 1992, A&A, 259, L39

McWilliam, A. 1997, ARA&A, 35, 503

Michaud, G., Vauclair, G., & Vauclair, S. 1983, ApJ, 267, 256

Moehler, S. 2001, PASP, 113, 1162

Moehler, S., Heber, U., Lemke, M., & Napiwotzki, R. 1998, A&A, 339, 537

Moehler, S., Sweigart, A. V., Landsman, W. B., Heber, U., & Catelan, M. 1999, A&A, 346, L1

Mooney, C. J., Rolleston, W. R. J., Keenan, F. P., et al. 2001, MNRAS, 326, 1101

Norris, J., & Freeman, K. C. 1983, ApJ, 266, 130

Paltrinieri, B., Ferraro, F. R., Paresce, F., & De Marchi, G. 2001, AJ, 121, 3114

Peterson, R., & Cudworth, K. M. 1994, ApJ, 420, 612

Ramirez, S. V., & Cohen, J. G. 2002, AJ, 123, 3277

Ramirez, S. V., & Cohen, J. G. 2003, AJ, 125, 224

Reyniers, M., & van Winckel, H. 2003, A&A, 408, L33

Rutledge, G. A., Hesser, J. E., Stetson, P. B., et al. 1997, PASP, 109, 883

Salaris, M., & Weiss, A. 2002, A&A, 388, 492

Sandage, A., & Smith, L. L. 1966, ApJ, 144, 886

Sneden, C. 1973, Ph.D. Thesis, Uniserity of Texas

Sneden, C. 1999, Ap&SS, 265, 145

Sneden, C., Pilachowski, C. A., & Kraft, R. P. 1997a, AJ, 120, 1351

Sneden, C., Kraft, R. P., & Shetrone, M. D. 1997b, AJ, 114, 1964

Sneden, C., Johnson, J., & Kraft, R. P., et al. 2000a, ApJ, 536, L85

Sneden, C., Pilachowski, C. A., & Kraft, R. P. 2000b, ApJ, 120, 1351

Sweigart, A. V., & Gross, P. G. 1974, ApJ, 190, 101

Thévenin, F. 1989, A&A, 77, 137

Thévenin, F. 1990, A&A, 82, 179

Thévenin, F., & Idiart, T. 1999, ApJ, 521, 753

Thévenin, F., Charbonnel, C., de Freitas Pacheco, J. A., et al. 2001, A&A, 373, 905

Thoul, A., Jorissen, A., Goriely, S., et al. 2002, A&A, 383, 491

Ventura, P., D'Antona, F., & Mazzitelli, I. 2002, A&A, 393, 215

Von Braun, K., Mateo, M., Chiboucas, K., Athey, A., & Hurley-Keller, D. 2002, AJ, 124, 2067

Wallerstein, G., Leep, E. M., & Oke, J. B. 1987, AJ, 93, 1137

Webbink, R. F. 1981, ApJS, 45, 259

Zinn, R. 1974, ApJ, 193, 593

Zinn, R., & West, M. J. 1984, ApJS, 55, 45

Zinn, R. J., Newell, E. B., & Gibson, J. B. 1972, A&A, 18, 390

Online Material

APPENDIX

NGC 5986

Star ID6 (star 1 in Table 4)

From the $B - V$ photometry of Alves et al. (2001) given in Tables 1 and 3, we derive T_{eff} = 9350 K or 9975 K respectively for a giant or a supergiant in using the calibration of Flower (1996). This calibration is adapted for population I stars, so these photometric T_{eff} are rough and have only been taken as starting values for the chemical analysis. From our analysis of the spectrum of this star we find T_{eff} = 8750 K.

From the analysis of the spectrum we derive [Fe/H] = −1.65, in good agreement with the mean metallicity of NGC 5986 ([Fe/H] = −1.61) determined by Kraft & Ivans (2003).

Since this work is the first chemical analysis of stars in NGC 5986, no comparison can be performed with abundances of other stars in the cluster.

We only note that in ID6:

- sodium and oxygen are slightly overabundant with respect to Fe, which is also the case for ZNG 1 in NGC 6712 (see Table 5). Ivans et al. (1999) find two giants among 32 in NGC 6121 (L2208 and L4201) showing similar overabundance of Na and O. For these stars Ivans et al. (1999) suggest primordial differences in the light element abundances and modest deep mixing. Statistics have to be improved in NGC 5986 before putting forward a similar hypothesis for ID6;
- absorption lines of s-elements are very weak or not present at all (see Fig. 2).

In Fig. 1 the star has a luminosity at the level of the tip of the AGB. From the location of the star in the HR diagram and its spectrum, we hypothesize that the star has evolved along the AGB sequence without experiencing the third dredge-up, and hence could be a PEAGB star.

Star ID7 (star 2 in Table 4)

The effective temperature of ID7 is lower by 2450 K than in ID6. As for ID6, the star shows overabundance of Na with regard to Fe (see Fig. 2). Oxygen is not detected in ID7. By means of our synthetic spectra we have established that the difference in temperature between ID6 and ID7 is sufficient to explain the non-detectability in ID7 of the OI lines, which have excitation energies higher than 9 eV. The metallicity of the star is only 0.2 dex lower than the mean value of the cluster, and thus probably not significant with regard to the accuracy (±0.1 dex) on our [Fe/H] determination (see Sect. 4.1). The significant differences between the chemical abundances of ID6 and ID7 are relative overabundances of some s-process elements in ID7.

The luminosity of ID7 is similar to ID6 (Table 4). Taking into account its location in the HR diagram (Fig. 1), we hypothesize that the star ID7 has probably evolved to the tip of the AGB and experienced the third dredge-up; this is supported by its s-process element abundance pattern. However we emphasize the lack of any published chemical analysis for a giant star in NGC 5986 that could strengthen our hypothesis. If the overabundance in s-elements is confirmed, ID7 could be a bona fide post-AGB star. The differences in the abundance patterns of ID6 and ID7 indicate that mixing and mass-loss processes and probably the initial main-sequence masses of these two stars were different.

NGC 6218 (Messier 12)

ZNG 7 (star 3 in Table 4)

Zinn et al. (1972) and Harris et al. (1983) list ZNG 7 as a UV-bright star in NGC 6218. From the old photographic photometry of the star (Table 3) and $E(B - V)$ of the cluster (Table 1), and from the T_{eff} calibration of Houdashelt et al. (2000) we derived T_{eff} = 5600 K. However from our detailed analysis of the spectrum of ZNG 7 we adopted T_{eff} = 4240 K.

The metallicity of ZNG 7 is [Fe/H] = −1.75 (Table 4), whereas mean [Fe/H] = −1.34 was found for NGC 6218 by Kraft & Ivans (2003). The metallicity scale ([Fe/H]) of Kraft & Ivans (2003) (based on FeII) is the best one up to now for the metallicity of globulars because it avoids errors due to overionization of FeI by a non-LTE effect (Thévenin & Idiart 1999). It supersedes the earlier scales of Zinn & West (1984), Carretta & Gratton (1997) and Rutledge et al. (1997) who gave, respectively, [Fe/H] = −1.61, −1.26 and −1.14 for NGC 6218. The underabundance of Fe in ZNG 7 compared to that of the cluster is about 0.4 dex and is significant with regard to our probable errors (±0.14 dex). What is the origin of this underabundance? It may be due to fractionation of some of the refractory elements into circumstellar dust. It is known that C, N, O, S, and Zn show almost solar photospheric abundances while Fe, Mg, Ca, Si, Cr, and other elements are very depleted relative to solar abundances (Mathis & Lamers 1992). The pattern of abundances of ZNG 7, especially the abundance of Zn ([Zn/Fe] = +0.22), is not similar to the interstellar and circumstellar pattern (see Fig. 3 in Jason & Cardelli 1984). This indicates that the lower [Fe/H] value of ZNG 7 is intrinsic and not due to condensation of Fe into the circumstellar dust. Moreover, there is no observational evidence for the presence of circumstellar dust around ZNG 7. Because the abundance analysis of Fe is based on FeI lines (the star is too cool to present FeII lines), Non-LTE overionization of FeI is strongly suspected. We have not found in the literature any abundance pattern of a giant star in NGC 6218. In Fig. 2 we have overplotted the abundance pattern of the UV-bright star ZNG 8 observed by Klochkova & Samus (2001). In ZNG 8 there is a large oxygen excess ([O/Fe] = 2.2), and overabundance of some alpha elements (Na, Si) which do not appear in ZNG 7.

In Fig. 1, we note that the luminosity of ZNG 7 is much lower than the tip of the AGB. The location of the star in the HR diagram very close to the AGB, indicates that it is a post-horizontal branch star and it may be evolving towards higher luminosity along the AGB.

NGC 6656 (Messier 22)

Star V-4 (star 4 in Table 4)

From the photometry of the star (Table 3), the interstellar extinction of NGC 6656 (Table 1) and the T_{eff} calibration of Houdashelt et al. (2000) we derive a $T_{\text{eff}} = 5250$ K for V-4, which is in good agreement with the $T_{\text{eff}} = 5500$ K derived from our spectral analysis.

The metallicity of V-4 ([Fe/H] = −1.78) is consistent with the mean metallicity of the cluster (Table 1). The chemical composition analysis of giants in NGC 6656 was carried out by Wallerstein et al. (1987), Lehnert et al. (1991) and Brown & Wallerstein (1992). For some of the giants in NGC 6656 Brown & Wallerstein (1992) found [Fe/H] = −1.78. According to Kraft (1994) there may be star-to-star variation of [Fe/H] as high as 0.1 dex in NGC 6656. In Fig. 3 we have also plotted the mean abundances of the CN-weak and CN-strong giant stars in NGC 6656 from Brown & Wallerstein (1992). The alpha elements in V-4 are in agreement with those CN-strong giants, but barium seems to be significantly overabundant with regard to these stars (see discussion in Sect. 5.2).

The position of the star in the HR diagram indicates that it is a post-HB star but not in a post-AGB evolutionary stage. Taking into account its abundance pattern, the star could have experienced third dredge-up episode, or may have been enriched in s-elements in some way (binarity or primordial scenario).

Star ZNG 5 (star 5 in Table 4)

The metallicity [Fe/H] of the star is in full agreement with the mean metallicity of the cluster. Alpha elements Ca and Ti are slightly overabundant compared to that of giants in NGC 6656 (see Fig. 2). The most important characteristic in ZNG 5 is the strong enhancement of the r-process element europium. Though the structure of the envelope of a star with $T_{\text{eff}} = 7450$ K and $\log g = 1.4$ is not available in the literature, we can expect a convective zone deep enough in ZNG 5 to prevent any diffusion effects. The most probable hypothesis is that the enhancements of all elements mentioned above, which are produced by supernovae (see Mc William 1997), are coming from pre-stellar material or later pollution.

There is no indication of overabundance of s-process elements in ZNG 5. Other chemical analyses are needed in order to further understand its abundance pattern. Its luminosity – one magnitude above the HB – seems to indicate that it is a post-HB star similar to V-4.

NGC 6712

Star ZNG 1 (star 6 in Table 4)

From the analysis of the spectrum of ZNG1 in NGC 6712 we find $T_{\text{eff}} = 11500$ K and [Fe/H] = −1.2, in agreement with the mean metallicity of NGC 6712 ([Fe/H] = −1.10, Kraft & Ivans 2003). Once more, we have not found any published chemical abundances of giant stars in NGC 6712 for comparison. In ZNG 1 we detect some even-Z elements (O, Mg, Si, Ti),

Ti being significantly underabundant relative to Fe (see Table 5). Most of the heavy elements beyond the iron peak, with nuclear charge $Z \geq 31$ are not detected.

The position on the evolutionary tracks of Dorman et al. (1993) indicates that ZNG 1 could be a PEAGB star on a rapid evolutionary loop.

NGC 7078 (Messier 15)

Star K 260 (star 7 in Table 4)

For this star we find $T_{\text{eff}} = 5250$ K and [Fe/H] = −2.5. Our results are in agreement with the temperature (5250 K), gravity (1.70) derived by Sneden et al. (2000b) by means of medium-resolution spectra.

The metallicity of K 260 is in agreement with the average metallicity of the cluster: [Fe/H] = −2.40 and [Fe/H] = −2.45 derived respectively by Sneden et al. (1997a) and Kraft & Ivans (2003). In Fig. 2 we compare the abundances relative to iron of K 260 with the giant star K 341 observed by Sneden et al. (1997a, 2000a,b). Relative to K 341, the UV-bright star K 260 shows significant overabundance of sodium and slight underabundance of magnesium. But Sneden et al. (1997a) find significant star-to-star variations in the abundances of oxygen, sodium, magnesium, aluminum, and neutron capture elements barium and europium in their sample of 18 bright giants in NGC 7078. They find that the oxygen and sodium abundances are strongly anticorrelated, while magnesium abundances are correlated. Hence the overabundance of Na and underabundance of Mg in K 260 are not inconsistent with the Mg-Na anticorrelation among giants in NGC 7078. We also note that in K 260, Sc is slightly enhanced with regard to the cluster mean abundance ([Sc/Fe] = −0.13, Sneden et al. 1997a).

In summary K 260 does not exhibit special chemical characteristics with regard to giants in NGC 7078. According to its location in the HR diagram (Fig. 1), the star may be a post-HB star.

Star K 996 (star 8 in Table 4)

We estimate the T_{eff} and luminosity of K 996 to be 11 500 K and 330 $L_{\odot}$ respectively. The values (10 000 ± 500 K and 250 $L_{\odot}$) derived by Cacciari et al. (1984) from IUE-calibrated UV fluxes are roughly consistent with our results. In the spectrum of K 996 we find very few absorption lines. Therefore the [Fe/H] value of K 996 may be uncertain. We find one line of MgII and two lines of SiII (see Tables 5 and 6). We have not found He lines in the spectrum of K 996 indicating possible underabundance of He as a result of diffusion, similar to that found in blue HB stars.

The position of K 996 on the evolutionary tracks of Dorman et al. (1993) indicates that it is probably a post-HB star. Cacciari et al. (1984) also suspected K 996 to be a star with a very hot HB progenitor and leaving the asymptotic giant branch in an early phase of AGB evolution or a star undergoing a loop away from the red giant branch.

Star K 1082 (star 9 in Table 4)

K 1082 shows slight overabundance of some α-elements and underabundance of magnesium with respect to the giant star K 341. The overabundance of Fe by about 0.35 dex compared to the cluster mean metallicity, and the small overabundances of Ca, Sc and Ti (see Fig. 2) relative to K 341 are well above the errors (± 0.13 dex, see Sect. 5.1). We have not found any atmosphere model for a post-HB star in the literature including radiative effects. However K 1082 is located near the TAHB in Fig. 1 and seems to be less evolved than ZNG 5, and thus could have a thiner convective envelope. We can only hypothetize that the overabundances of some elements in the post-HB star K 1082 could be due to mild diffusion effects as in blue HB stars (see Michaud et al. 1983; Behr et al. 1999). Its luminosity is too low for the third dredge-up to have occured. The significant overabundance of some of the s-process elements may be due to star-to-star variation in NGC 7078, or K 1082 may be a hotter, evolved analogue of a barium star.